Neutrosophic Sets and Systems, Vol. 76, 2025
University of New Mexico

An Evaluation Method for University Classroom Education Quality under Machine Vision and Single-Valued Neutrosophic Hesitant Fuzzy Set Environment

Rui Wang [1], Mingjie Li [1*] Fangwei Zhang [2], Yiying Pan [1] and Zongao Zhang[1]

[1] School of Navigation and Shipping, Shandong Jiaotong University, Weihai China.
Email: Rui Wangrui: wang27@163.com, Mingjie Li: 201046@sdjtu.edu.cn, Yiying Pan: yiyingpan02@163.com, Zongao Zhang: zongaozhang@163.com.
[2] School of International Business, Shandong Jiaotong University, Weihai China.
Email: Fangwei Zhang: fangweirzhang@163.com.
* Correspondence: 201046@sdjtu.edu.cn

Abstract: With the advancement of artificial intelligence, machine vision offers a novel approach to university teaching quality evaluation (TQE). However, existing studies are often hindered by subjectivity and lack of standardized evaluation methods, which impede accurate assessment of student learning effectiveness. Therefore, this study addresses these limitations by proposing a TQE framework that integrates machine vision with single-valued neutrosophic hesitant fuzzy sets (SVNHFSs). Specifically, the main contributions of this study are as follows. First, this study innovatively employs machine vision to capture student learning behaviors, constructing a classroom behavior matrix that serves as the foundation for evaluation. Second, this study introduces a combined weighting method, leveraging both the entropy weight method and the Criteria Importance Through Inter-Criteria Correlation (CRITIC) weight method, to assign weights to different time-points during the classes. Third, the SVNHFS is utilized to construct a classroom behavior evaluation matrix, and the single-valued neutrosophic hesitant fuzzy weighted average (SVNHFWA) operator is applied for weighting. In addition, the cosine measure is employed to rank time-points based on both ideal and non-ideal solutions, obtaining the optimal and non-optimal learning effectiveness periods. Finally, a case study confirms the effectiveness and feasibility of the proposed model, offering a robust method for evaluating university education quality.
Keywords: Teaching Quality Evaluation, Machine vision, Classroom Behavior Analysis, Single-valued neutrosophic hesitant fuzzy set, Hybrid Weighting Method, Multi-attribute decision-making.

1. Introduction

With the rapid advancement of artificial intelligence, machine vision is increasingly being utilized in teaching quality evaluation (TQE) at colleges and universities [1]. Traditional classroom evaluation methods often focus on superficial metrics, such as exam scores and attendance, which do not adequately capture students' learning outcomes or teachers' instructional effectiveness [2]. To overcome these limitations, educational institutions have begun incorporating video surveillance in classrooms to analyze both teaching activities and student behavior. This approach offers a more comprehensive and objective means of assessing teaching effectiveness within the TQE framework in higher education.

However, evaluating the quality of university education involves various or the same attributes, making the process of TQE a complex multi-attribute decision-making (MADM) problem [3]. The application of single-valued neutrosophic hesitant fuzzy sets (SVNHFSs) offers an effective approach to addressing this complexity [4]. Therefore, this study integrates machine vision with SVNHFS in the evaluation process, offering a novel perspective on TQE. To further explore the application of machine vision and SVNHFS in teaching evaluation, this study reviews relevant literature to provide theoretical support and practical guidance.

In recent years, scholars have focused on improving the effectiveness and accuracy of TQE [5-8]. For example, Li and Zhang employed big data, integrating K-means clustering and Apriori algorithms, to monitor and improve teaching quality in higher education, achieving more precise evaluations and enhancements [9]. Xia employed the probabilistic hesitant fuzzy TODIM-EDAS technique combined with the CRITIC method, thereby supporting institutions in cultivating more international technical talents [10]. Ahmad et al. proposed a machine learning-optimized TQE framework, which offers a more precise and systematic approach to assessing teaching quality by analyzing teacher performance in e-learning environments [11]. Cui proposed the artificial bee colony optimization algorithm combined with a classification and regression tree model to enhance TQE, significantly improving accuracy and generalizability through AI-driven methods [12]. Li and Wang proposed a TQE framework based on 5G and edge computing technologies, which significantly enhances the efficiency and accuracy of teaching quality assessments, thereby strengthening educational management [13]. Zhao et al. developed a blended teaching quality evaluation scale for nursing education based on the Context, Input, Process, and Product (CIPP) model, enhancing the reliability and validity of teaching TQE [14]. Ren et al. utilized deep learning and dictionary-based techniques for aspect-level sentiment analysis of student feedback, thereby enhancing the objectivity and depth of teaching quality evaluation [15].

Meanwhile, the neutrosophic set (NS) is a foundational tool for addressing uncertainty and inconsistency in MADM problems, with applications across various fields [16-18]. Numerous extensions of NSs have been developed to further enhance its capability in handling more complex decision-making scenarios [19]. For instance, Saqlain et al. introduced a multi-polar interval-valued neutrosophic hypersoft set model, which employs distance and similarity measures to address uncertainty in complex MADM problems [20]. Then, Florentin introduced the SuperHyperSoft Set and its fuzzy extension, expanding the Soft Set theory to address complex decision-making scenarios with greater flexibility and inclusivity of uncertainties and inconsistencies [21]. Meanwhile, Zhao and Ye proposed a MADM model combining Simplified NS and TOPSIS, improving the TQE framework's accuracy and reliability by handling uncertainties and inconsistencies in evaluations [22]. And Ye proposed a MADM method based on the SVNHFS, which effectively deals with the uncertainty and hesitation in the decision by developing new aggregation operators and measurement functions [23]. Building on such advancements, Muhammad et al. investigated the efficiency of wastewater treatment using interval-valued neutrosophic fuzzy soft sets, offering a systematic approach to ensure the security and quality of drinking water by incorporating distance measures [24]. Ahmed et al. introduced a neutrosophic MCDM model to assess sustainable soil enhancement in construction, highlighting lifecycle assessment's importance for sustainable practices and cost analysis [25].

Besides, with the development of AI, machine vision has become an excellent decision-aid tool in various fields [26-28]. Bai et al. integrated an enhanced YOLOv4 with MobileNetV3 to develop an efficient machine vision approach for detecting surface defects on railway tracks, achieving a lightweight network and rapid, accurate identification [29]. Zhang et al. presented an enhanced YOLOv4-Tiny model for weed detection in peanut fields, offering a valuable tool for precision agriculture [30]. Then, shifting focus to the TQE field, Li et al. developed an objective and precise TQE evaluation method using machine vision and Fermatean fuzzy sets, enhancing both the objectivity and efficiency of the evaluation [31]. Bai proposed a teaching system based on machine vision and sensor audio signal processing, aiming to improve students' learning outcomes in musical performance skills [32]. Cheng obtained the evaluation of classroom activity through student expression and posture recognition and realized student classroom teaching automatic acquisition [33]. Goldberg et al. proposed an action recognition method based on machine vision, which effectively evaluates the visible engagement of college students in classroom teaching [34].

Considering the above reference reviews, research on TQE has made noteworthy progress, and the application of SVNHFS and machine vision in many fields is also extensive. But there are still some aspects that need considering as follows.

1) Traditional teaching evaluation methods rely on subjective decisions from evaluators, resulting in objectivity issues and lower efficiency. There is a need for more objective and streamlined evaluation methods.

2) Despite the wide application of machine vision in various fields, its use in the TQE remains underdeveloped, and methods integrating this technology require further refinement.

3) While SVNHFS offers a new perspective for addressing MADM problems, current research still needs improvement. Given the complexity and challenges of TQE, there is no unified framework to address these issues effectively.

Based on the aforementioned, the motivation of this study is to propose an objective and precise TQE framework that integrates SVNHFS with machine vision to minimize subjectivity in the evaluation process. Then, this study proposes an evaluation method for TQE in machine vision and SVNHFS environment. The primary contributions of this study are summarized as follows.

First, this study adopts the objective detection algorithm based on deep learning, YOLOv5, to detect different classroom learning behaviors during teaching time. Then, based on these learning behaviors, a learning behavior matrix is constructed. This approach enhances the objectivity of behavior detection and provides a novel approach to the TQE process.

Second, this study employs a combined weighting approach using the entropy weight method and the CRITIC method to determine the weights at specific time points. This approach replaces the subjective weighting process, mitigating the limitations of single-method weighting, and enhancing the objectivity and effectiveness of the TQE process.

Third, this study constructs time-based SVNHF evaluation matrices to assess students' classroom behaviors at specific intervals. The classical SVNHFWA operator is then employed, using the weights derived from the combined weighting method to ensure a balanced and accurate evaluation of each time point.

Additionally, this study employs the SVNHFS cosine measure operators to rank the time-points based on the learning effect and inspired by the SVNHFS cosine measure operator, a negative cosine measure operator is introduced for the non-ideal SVNHFE. By incorporating both cosine measure values, the TQE process is more comprehensive. For ease of understanding, Figure 1 gives the main framework of this study.

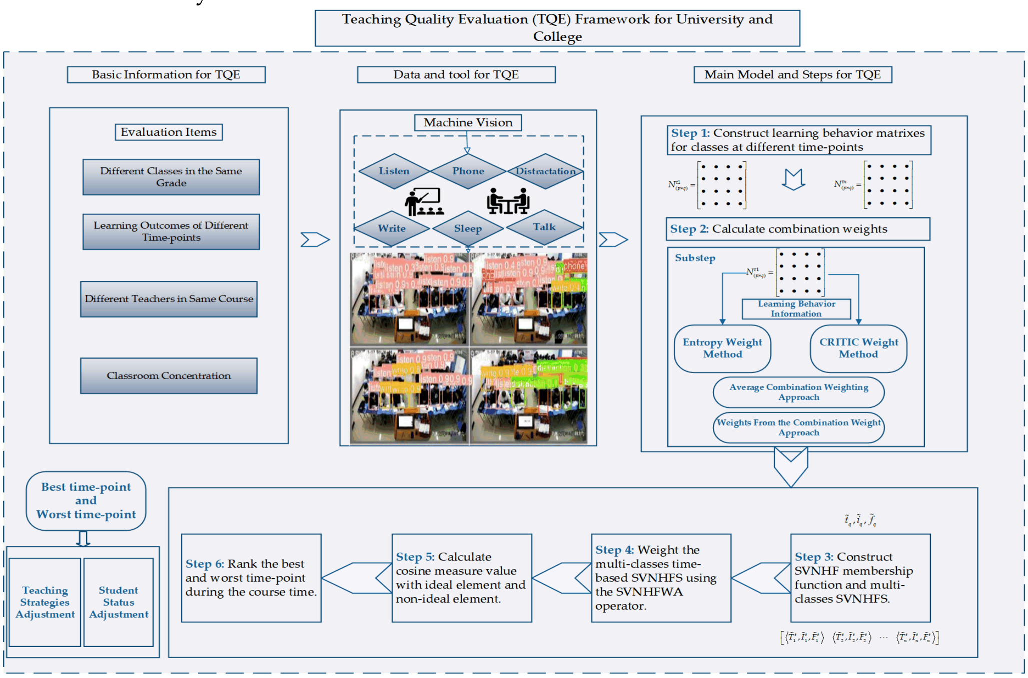

Figure 1. The main framework of this study.

The remainder of this study is structured as follows. Section 2 provides a brief introduction to the related concepts of SVNHFSs. Section 3 presents a framework for university TQE that combines SVNHFSs and machine vision. In Section 4, the classroom evaluation decision model proposed in this study is validated through a case example, and the results obtained are analyzed and discussed. In Section 5, the conclusion of this study is summarized.

2. Preliminary studies

In the general concept, an SVNHFS is the combination of the hesitant fuzzy set (HFS) and SVNS [35]. Specifically, there are some basic concepts of SVNHFS as follows.

Definition 1 [35]. Let X be a fixed set C, and the elements of X are represented by x. Then, the SVNHFS is defined as

$$C=\left\{\left\langle x,\tilde{T}_C\left(x\right),\tilde{I}_C\left(x\right),\tilde{F}_C\left(x\right)\right\rangle\middle|x\in X\right\},$$

where $\tilde{T}_C(x)$, $\tilde{I}_C(x)$, and $\tilde{F}_C(x)$ are defined as the possible truth-membership hesitant degrees, indeterminacy-membership hesitant degrees, and falsity-membership hesitant degrees, respectively. Whereas $\tilde{T}_C(x)$, $\tilde{I}_C(x)$, and $F(x) \in [0,1]$ for each element x in X to the fixed set C. Besides, the SVNHFS has the following conditions.

1). $\alpha, \beta, \gamma \in [0,1]$, where the $\alpha \in \tilde{T}_C(x)$, $\beta \in \tilde{I}_C(x)$, $\gamma \in \tilde{F}_C(x)$.

2). $\alpha^+ \oplus \beta^+ \oplus \gamma^+ \in [0,3]$, where $\alpha^+ \in \tilde{T}_C^+(x) = \cup_{\alpha^+ \in \tilde{T}_C(x)} max\{\alpha\}$, $\beta^+ \in \tilde{I}_C^+(x) = \cup_{\beta^+ \in \tilde{I}_C(x)} max\{\beta\}$, $\gamma^+ \in \tilde{F}_C^+(x) = \cup_{\gamma^+ \in \tilde{F}_C(x)} max\{\gamma\}$. Specifically, α^+, β^+, γ^+ represent the maximum value of $\tilde{T}_C^+(x)$, $\tilde{I}_C^+(x)$, and $\tilde{F}_C^+(x)$, respectively.

For convenience, the three tuples $c(x) = \{\tilde{T}_C(x), \tilde{I}_C(x), \tilde{F}_C(x)\}$ is described as single-value neutrosophic hesitant fuzzy element (SVNHFE), which is easily denoted as $c = \{\tilde{T}, \tilde{I}, \tilde{F}\}$.

Then, the related relations between two SVNHFEs are as follows.

Definition 2 [35]. Let $c_1 = \{\tilde{T}_1, \tilde{I}_1, \tilde{F}_1\}$ and $c_2 = \{\tilde{T}_2, \tilde{I}_2, \tilde{F}_2\}$ be two SVNHFEs in a fixed set X, it gets the following relations.

1). $c_1 \cup c_2 = \{\tilde{T} \in (\tilde{T}_1 \cup \tilde{T}_2) | \tilde{T} \geq max(\tilde{T}_1^-, \tilde{T}_2^-), \tilde{I} \in (\tilde{I}_1 \cap \tilde{I}_2) | \tilde{I} \leq min(\tilde{I}_1^-, \tilde{I}_2^-), \tilde{F} \in (\tilde{F}_1 \cap \tilde{F}_2) | \tilde{F} \leq min(\tilde{F}_1^-, \tilde{F}_2^-)\}$.

2). $c_1 \cap c_2 = \{\tilde{T} \in (\tilde{T}_1 \cap \tilde{T}_2) | \tilde{T} \leq min(\tilde{T}_1^+, \tilde{T}_2^+), \tilde{I} \in (\tilde{I}_1 \cup \tilde{I}_2) | \tilde{I} \geq max(\tilde{I}_1^+, \tilde{I}_2^+), \tilde{F} \in (\tilde{F}_1 \cup \tilde{F}_2) | \tilde{F} \geq max(\tilde{F}_1^+, \tilde{F}_2^+)\}$.

Since, the basic operations for two SVNHFEs are given as follows.

Definition 3 [35]. Let c_1 and c_2 be two SVNHFEs in a fixed set X. It gets the following operations.

1. $c_1 \oplus c_2 = \{\tilde{T}_1 \oplus \tilde{T}_2, \tilde{I}_1 \otimes \tilde{I}_2, \tilde{F}_1 \otimes \tilde{F}_2 = U_{\alpha_1 \in \tilde{T}_1, \beta_1 \in \tilde{I}_1, \gamma_1 \in \tilde{F}_1, \alpha_2 \in \tilde{T}_2, \beta_2 \in \tilde{I}_2, \gamma_2 \in \tilde{F}_2}\{\{\alpha_1 + \alpha_2 - \alpha_1\alpha_2\}, \{\beta_1\beta_2\}, \{\gamma_1\gamma_2\}\}$.
2. $c_1 \otimes c_2 = \{\tilde{T}_1 \otimes \tilde{T}_2, \tilde{I}_1 \oplus \tilde{I}_2, \tilde{F}_1 \oplus \tilde{F}_2 = U_{\alpha_1 \in \tilde{T}_1, \beta_1 \in \tilde{I}_1, \gamma_1 \in \tilde{F}_1, \alpha_2 \in \tilde{T}_2, \beta_2 \in \tilde{I}_2, \gamma_2 \in \tilde{F}_2}\{\{\alpha_1\alpha_2\}, \{\beta_1 + \beta_2 - \beta_1\beta_2\}, \{\gamma_1 + \gamma_2 - \gamma_1\gamma_2\}\}$.
3. $\lambda c_1 = \{U_{\alpha_1 \in \tilde{T}_1, \beta_1 \in \tilde{I}_1, \gamma_1 \in \tilde{F}_1}\{\{1 - (1 - \alpha_1)^\lambda\}, \{\beta_1{}^\lambda\}, \{\gamma_1{}^\lambda\}\}, \lambda > 0$.
4. $c_1{}^\lambda = \{U_{\alpha_1 \in \tilde{T}_1, \beta_1 \in \tilde{I}_1, \gamma_1 \in \tilde{F}_1}\{\{\alpha_1{}^\lambda\}, \{1 - (1 - \beta_1)^\lambda\}, \{1 - (1 - \gamma_1)^\lambda\}\}, \lambda > 0$.

Based on the SVNSs cosine measure method [28], the SVNHFEs cosine measure method is obtained as follows.

Definition 4 [35]. Let $c_1 = \{\tilde{T}_1, \tilde{I}_1, \tilde{F}_1\}$ and $c_2 = \{\tilde{T}_2, \tilde{I}_2, \tilde{F}_2\}$ be two SVNHFEs in a fixed set X. Therefore, the SVNHFEs cosine measure method is defined as follows.

$$\cos\left(c_1,c_2\right)=\frac{\left(\frac{1}{\delta_1}\sum_{\alpha_1\in\tilde{T}_1}\alpha_1\right)\cdot\left(\frac{1}{\delta_2}\sum_{\alpha_2\in\tilde{T}_2}\alpha_2\right)+\left(\frac{1}{\varepsilon_1}\sum_{\beta_1\in\tilde{I}_1}\beta_1\right)\cdot\left(\frac{1}{\varepsilon_2}\sum_{\beta_2\in\tilde{I}_2}\beta_2\right)+\left(\frac{1}{\eta_1}\sum_{\gamma_1\in\tilde{F}_2}\gamma_1\right)\cdot\left(\frac{1}{\eta_2}\sum_{\gamma_2\in\tilde{F}_2}\gamma_2\right)}{\sqrt{\left(\frac{1}{\delta_1}\sum_{\alpha_1\in\tilde{T}_1}\alpha_1\right)^2+\left(\frac{1}{\varepsilon_1}\sum_{\beta_1\in\tilde{I}_1}\beta_1\right)^2+\left(\frac{1}{\eta_1}\sum_{\gamma_1\in\tilde{F}_2}\gamma_1\right)^2}\cdot\sqrt{\left(\frac{1}{\delta_2}\sum_{\alpha_2\in\tilde{T}_2}\alpha_2\right)^2+\left(\frac{1}{\varepsilon_2}\sum_{\beta_2\in\tilde{I}_2}\beta_2\right)^2+\left(\frac{1}{\eta_2}\sum_{\gamma_2\in\tilde{F}_2}\gamma_2\right)^2}},\quad(1)$$

where $\delta, \varepsilon, \eta$ represent the numbers of the elements in $\tilde{T}$, $\tilde{I}$, $\tilde{F}$, respectively. And the $\cos(c_1, c_2) \in [0,1]$. Thus, based on the SVNHFEs cosine measure method, the cosine measure between $c_i (i = 1,2)$ and ideal element $c^* =< 1,0,0 >$ is obtained as follows.

$$\cos\left(c_i,c^*\right)=\frac{\left(\frac{1}{\delta_i}\sum_{\alpha_i\in\tilde{T}_i}\alpha_i\right)}{\sqrt{\left(\frac{1}{\delta_i}\sum_{\alpha_i\in\tilde{T}_i}\alpha_i\right)^2+\left(\frac{1}{\varepsilon_i}\sum_{\beta_i\in\tilde{I}_i}\beta_i\right)^2+\left(\frac{1}{\eta_i}\sum_{\gamma_i\in\tilde{F}_i}\gamma_i\right)^2}}. \tag{2}$$

Similarly, where $\delta_i,\varepsilon_i,\eta_i,(i=[1,2])$ represent the numbers of the elements in $\tilde{T}_i$, $\tilde{I}_i$, $\tilde{F}_i$, respectively. And the $\cos(c_i,c^*)\in[0,1], i=[1,2]$. Since, the SVNHFEs' cosine measure comparative laws are obtained as follows.

1) If $\cos(c_1,c^*)>\cos(c_2,c^*)$, then $c_1\succ c_2$.
2) If $\cos(c_1,c^*)=\cos(c_2,c^*)$, then $c_1\sim c_2$.

3. Evaluation Methods of University Classroom Education

In this section, to better evaluate the university classroom students' learning effect, this study proposes an evaluation framework for TQE in machine vision and SVNHFS environment. The specific steps are as follows.

Step 1. In this step, this study uses q types of behaviors identified by the YOLOv5 object detection algorithm as the columns of the matrix. Then, the total duration of the course is equally divided into p segments, serving as the rows of the time-based learning behaviors matrix. Therefore, the matrix is obtained as follows.

$$N^t_{(p\times q)}=\begin{bmatrix} n_{11} & n_{12} & \cdots & n_{1q}\\ n_{21} & n_{22} & \cdots & n_{2q}\\ \vdots & \vdots & \ddots & \vdots\\ n_{p1} & n_{p2} & \cdots & n_{pq}\end{bmatrix},$$

where $N^t_{(p\times q)}$ represents the multi-classes learning behaviors matrix, $t=(1,2,\cdots,t)$ represents the time point, and $n_{pq}, p=(1,2,\cdots,p), q=(1,2,\cdots,q)$ represents the number of students in class p with learning behavior q.

Step 2. In this step, based on the combination of the classical entropy weight method and CRITIC weight method, the way of combined weighting method is adopted to obtain the weights under different classes and behaviors. The specific sub-steps are as follows.

Step 1'. Calculate the proportion of each behavior in each class p_{ij}. Then, p_{ij} is defined as follows.

$$p_{ij}=\frac{n_{pq}}{\sum_{p=1}^{p}n_{pq}}. \tag{3}$$

Next, calculate each behavior information entropy $e_j,(j=1,2,\cdots,q)$ for each behavior. Then, e_j is defined as follows.

$$e_j=-\frac{1}{\ln p}\sum_{i=1}^{p}p_{ij}\ln p_{ij}, \tag{4}$$

where $\boldsymbol{\frac{1}{lnp}>0, e_j\geq 0}$.

Step 2'. Calculate the weights of each behavior through the behavior information entropy. Then, the weight of each behavior $\boldsymbol{w_j,(j=1,2,\cdots,q)}$ is obtained as follows.

$$w_j=\frac{1+\frac{1}{\ln p}\sum_{i=1}^{p}p_{ij}\ln p_{ij}}{\sum_{j=1}^{q}1-\left(-\frac{1}{\ln p}\sum_{i=1}^{p}p_{ij}\ln p_{ij}\right)}. \tag{5}$$

Step 3'. Therefore, each class comprehensive score $\boldsymbol{S_{1i}}$ is obtained by the learning behaviors matrix $\mathbf{N}^{\boldsymbol{t}}_{(\boldsymbol{p}\times\boldsymbol{q})}$ and weight of each behavior $\boldsymbol{w_j}$. Then, it gets

$$S_{1i} = \sum_{j=1}^{q} \sum_{q=1}^{q} w_j \cdot n_{pq}. \tag{6}$$

Each class gets its weight at time-point t. Then, it gets

$$w_{ei} = \frac{S_{1i}}{\sum_{i=1}^{p} S_{1i}}. \tag{7}$$

Thus, the weight vector of each class at time-point *t* using the entropy weight method is obtained as $w_e^t = [w_{e1}, w_{e1}, \cdots, w_{ep}]$.

Step 4'. Based on the learning behaviors matrix $\mathbf{N}_{(p\times q)}^t$, the Pearson correlation coefficient matrix is obtained by the Pearson correlation coefficient r_{pq} [36]. Thus, the indicator conflict in learning behavior is obtained as follows.

$$R_j = \sum_{p=1}^{p} 1 - r_{pq}. \tag{8}$$

Thus, the amount of information about learning behavior C_q is obtained as follows.

$$C_q = \delta_q \sum_{p=1}^{p} 1 - r_{pq}, \tag{9}$$

where δ_q represents the standard deviation of learning behavior *q*. Meanwhile, the larger C_q is, the more significant the role of the *q*th learning behavior index in the overall evaluation process.

Step 5'. Thereafter, the CRITIC weight of each behavior $w_{2j}, (j = 1, 2, \cdots, q)$ is obtained as follows.

$$w_{2q} = \frac{C_q}{\sum_{q=1}^{q} C_q}. \tag{10}$$

Step 6'. Therefore, each class comprehensive score S_{2i} is obtained by $\mathbf{N}_{(p\times q)}^t$ and w_{2q}. It gets

$$S_{2i} = \sum_{q=1}^{q} w_q^t \cdot n_{pq}. \tag{11}$$

Thereafter, each class gets its weight at time-point t. It gets

$$w_{ci}^t = \frac{S_{2i}^t}{\sum_{i=1}^{p} S_{2i}^t}. \tag{12}$$

Then, the weight vector of each class at time-point *t* using the CRITIC weight method is obtained as $w_c^t = [w_{c1}, w_{c1}, \cdots, w_{cp}]$.

Step 7'. This study adopts the weighted average method. Therefore, the combined weight in the weighted average method is defined as follows.

$$W_i = \theta w_{ei} + (1-\theta) w_{ci}, \tag{13}$$

where $W = (W_1, W_2, \cdots, W_i)^{\mathrm{T}}$ is the combined weight vector in the weighted average method, and $\theta = 0.5$.

Step 3. For convenience, based on the q classroom learning behaviors identified by YOLOv5, classify the different learning behaviors into truth-membership, indeterminacy-membership, and falsity-membership. Therefore, this study gives the truth-membership hesitant degree $\tilde{t}_q$, indeterminacy-membership hesitant degree $\tilde{\imath}_q$, and falsity-membership $\tilde{f}_q$ as follows.

$$\tilde{t}_q = \frac{\sum_{q=1}^{n} b_q}{\sum_{q=1}^{q} b_q}, q = \{1, 2, \dots, n\}, \tag{14}$$

$$\tilde{i}_q = \frac{b_q}{\sum_{q=1}^{q} b_q}, q = \{n+1, n+2, ..., m\}, \tag{15}$$

$$\tilde{f}_q = \frac{b_q}{\sum_{i=1}^{q} b_q}, q = \{m+1, m+2, ..., q\}, \tag{16}$$

where $b_q, q = (1, 2, \cdots, n, n+1, \cdots, m, m+1, \cdots, q)$ represents the classroom learning behavior.

Therefore, class one for the time-based SVNHFS U_1 is obtained as follows.

$$U_1^t = \left\langle \tilde{T}_1^t, \tilde{I}_1^t, \tilde{F}_1^t \right\rangle$$
$$= \left\langle \{\tilde{t}_1^t, \tilde{t}_2^t, \cdots, \tilde{t}_q^t\}, \{\tilde{i}_1^t, \tilde{i}_2^t, \cdots, \tilde{i}_q^t\}, \{\tilde{f}_1^t, \tilde{f}_2^t, \cdots, \tilde{f}_q^t\} \right\rangle.$$

However, since the subject of this study is classroom education quality assessment in multiple classes, the multi-classes SVNHFS at time-point t is obtained as follows.

$$U^t = \begin{bmatrix} U_1^t & U_2^t & \cdots & U_n^t \end{bmatrix}$$
$$= \begin{bmatrix} \left\langle \tilde{T}_1^t, \tilde{I}_1^t, \tilde{F}_1^t \right\rangle & \left\langle \tilde{T}_2^t, \tilde{I}_2^t, \tilde{F}_2^t \right\rangle & \cdots & \left\langle \tilde{T}_n^t, \tilde{I}_n^t, \tilde{F}_n^t \right\rangle \end{bmatrix}.$$

Step 4. To reflect the importance of each learning behavior more accurately and reasonably in the process of MADM of classroom education quality. This study weights the multi-classes time-based SVNHFS by the SVNHFWA operator. Specifically, aggregate all multi-classes time-based SVNHFEs of U_{tn} by the SVNHFWA operator. Then, the collective SVNHFE U_t for a time point $t\ (t = 1, 2, \cdots, t)$ is obtained as follows.

$$\phi_t = SVNHFWA\left(U_1^t, U_2^t, \cdots U_n^t\right) = \sum_{n=1}^{n} W^t \cdot U_n^t$$
$$= \bigcup_{\tilde{t}_1^t \in \tilde{T}_1^t, \cdots, \tilde{t}_q^t \in \tilde{T}_q^t, \tilde{i}_1^t \in \tilde{I}_1^t, \cdots, \tilde{i}_q^t \in \tilde{I}_q^t, \tilde{f}_1^t \in \tilde{F}_1^t, \cdots, \tilde{f}_q^t \in \tilde{F}_q^t} \left\{ \left\{ 1 - \prod_{q=1}^{q} \left(1 - \tilde{t}_q^t\right)^{W^t} \right\}, \left\{ \prod_{q=1}^{q} \left(1 - \tilde{i}_q^t\right)^{W^t} \right\}, \left\{ \prod_{q=1}^{q} \left(1 - \tilde{f}_q^t\right)^{W^t} \right\} \right\} \tag{17}$$

Step 5. From **Def. 4**, the classical cosine measure method calculates the value between the SVNHFEs and ideal element $U^* =< 1, 0, 0 >$. However, the imperfect element $U^- =< 0, 0, 1 >$ also reflects the solution's quality. Thus, based on the SVNHFEs cosine measure method, the cosine measure between SVNHFEs and imperfect element $U^- =< 0, 0, 1 >$ is obtained as follows.

$$\cos\left(\phi_i, \phi^-\right) = \frac{\left(\frac{1}{\tilde{f}_i} \sum_{\tilde{f}_i \in \tilde{F}_i} \tilde{f}_i\right)}{\sqrt{\left(\frac{1}{\tilde{t}_i} \sum_{\tilde{t}_i \in \tilde{T}_i} \tilde{t}_i\right)^2 + \left(\frac{1}{\tilde{i}_i} \sum_{\tilde{i}_i \in \tilde{I}_i} \tilde{i}_i\right)^2 + \left(\frac{1}{\tilde{f}_i} \sum_{\tilde{f}_i \in \tilde{F}_i} \tilde{f}_i\right)^2}}. \tag{18}$$

Step 6. Calculate the positive cosine measurement values between $U_t\ (t = 1, 2, \cdots, t)$ and $U^* = < 1, 0, 0 >$ by Eq. (2), and negative cosine measurement value between $U_t\ (t = 1, 2, \cdots, t)$ and the non-ideal element $U^- =< 0, 0, 1 >$ by Eq. (18). Finally, rank the best and worst time point(s), respectively.

4. Results and Discussion

Firstly, in this section, this study introduces the dataset used for training the YOLOv5 learning behaviors detection algorithm. Secondly, this study gives a practical case application to validate the effectiveness of the proposed model. Thirdly, this study gives a comprehensive analysis and discussions of the obtained results.

4.1. Data Set Description

Object detection and recognition are fundamental technologies in machine vision, enabling the identification of specific objects in images or videos and the extraction of relevant information about these objects [37]. This study employs detection and recognition techniques based on the YOLOv5 framework to identify four categories of student behavior in the 'Advanced Mathematics' course, and to construct the corresponding dataset.

A large volume of videos featuring undergraduate students from various majors and academic years was collected using classroom-facing cameras. To facilitate processing, these instructional videos were segmented into individual frames, yielding a curated dataset of 2,000 viable images. Additionally, a Learning Behavior Dataset (LBDS) was developed by selecting and analyzing six common classroom behaviors through both manual investigation and online annotation using the Make Sense platform. Specifically, student behaviors were categorized as "listening, writing, using phones, sleeping, talking, and distraction." An example of the LBDS is shown in Figure 2.

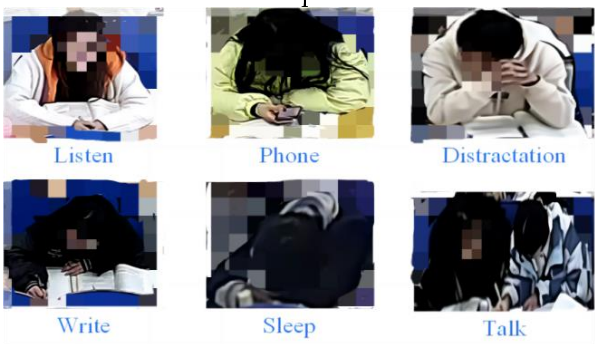

Figure 2. The example of LBDS.

In the experiment, the LBDS is divided into a training set and a testing set in a 4:1 ratio. The training set is used to train the detection model, while the testing set is employed for experimental validation. The study employs the controlled variable method in the comparative experiments, ensuring that all other factors remain constant when analyzing the network's detection accuracy and speed. The code in this study has been optimized by referencing the best parameter configurations from other network models. Ultimately, real-time counting of student behaviors in the classroom is achieved. After class, the real-time counting data is exported as an Excel file for subsequent data analysis. The recognition and analysis process is illustrated in Figure 3, and the results of classroom behavior recognition are shown in Figure 4.

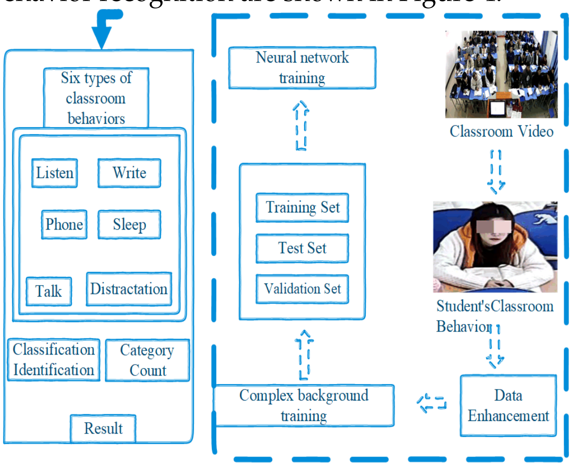

Figure 3. Student behavior identification and analysis process.

Figure 4. Effect Chart of Classroom Learning Recognition.

4.2. Case Study Application

In this subsection, the proposed model is applied in a case study. Specifically, this case study focuses on the "Advanced Mathematics" course across four classes, with each class lasting one hour. Meanwhile, this study divides the course duration into 9 time points equally. Thus, the detailed steps of the case application are shown as follows.

Step 1. Based on six learning behaviors identified by YOLOv5, four classes of learning behavior matrixes at 9 time points are established as follows.

$$N^{t1}=\begin{bmatrix} & listen & write & talk & distraction & phone & sleep \\ class1 & 20 & 5 & 3 & 2 & 1 & 2 \\ class2 & 18 & 3 & 4 & 3 & 6 & 1 \\ class3 & 15 & 2 & 5 & 3 & 5 & 1 \\ class4 & 21 & 6 & 5 & 4 & 6 & 2 \end{bmatrix},\ N^{t2}=\begin{bmatrix} & listen & write & talk & distraction & phone & sleep \\ class1 & 22 & 4 & 4 & 3 & 4 & 2 \\ class2 & 16 & 5 & 5 & 5 & 1 & 1 \\ class3 & 17 & 4 & 6 & 6 & 3 & 2 \\ class4 & 25 & 7 & 5 & 3 & 4 & 2 \end{bmatrix},$$

$$N^{t3}=\begin{bmatrix} & listen & write & talk & distraction & phone & sleep \\ class1 & 23 & 6 & 2 & 5 & 6 & 3 \\ class2 & 20 & 7 & 1 & 4 & 6 & 5 \\ class3 & 22 & 4 & 3 & 4 & 3 & 3 \\ class4 & 23 & 6 & 2 & 1 & 2 & 1 \end{bmatrix},\ N^{t4}=\begin{bmatrix} & listen & write & talk & distraction & phone & sleep \\ class1 & 21 & 6 & 3 & 2 & 3 & 2 \\ class2 & 25 & 5 & 2 & 2 & 5 & 3 \\ class3 & 19 & 3 & 2 & 3 & 5 & 6 \\ class4 & 26 & 8 & 3 & 2 & 3 & 1 \end{bmatrix},$$

$$N^{t5}=\begin{bmatrix} & listen & write & talk & distraction & phone & sleep \\ class1 & 19 & 8 & 5 & 4 & 4 & 2 \\ class2 & 10 & 2 & 4 & 3 & 7 & 4 \\ class3 & 13 & 2 & 5 & 4 & 6 & 4 \\ class4 & 25 & 5 & 2 & 4 & 2 & 2 \end{bmatrix},\ N^{t6}=\begin{bmatrix} & listen & write & talk & distraction & phone & sleep \\ class1 & 17 & 2 & 6 & 2 & 5 & 1 \\ class2 & 14 & 3 & 2 & 1 & 6 & 1 \\ class3 & 10 & 4 & 6 & 4 & 8 & 2 \\ class4 & 20 & 6 & 1 & 3 & 3 & 2 \end{bmatrix},$$

$$N^{t7}=\begin{bmatrix} & listen & write & talk & distraction & phone & sleep \\ class1 & 18 & 3 & 7 & 4 & 6 & 1 \\ class2 & 12 & 2 & 3 & 2 & 7 & 3 \\ class3 & 12 & 5 & 6 & 3 & 5 & 5 \\ class4 & 18 & 7 & 4 & 2 & 5 & 1 \end{bmatrix},\ N^{t8}=\begin{bmatrix} & listen & write & talk & distraction & phone & sleep \\ class1 & 15 & 4 & 6 & 3 & 6 & 2 \\ class2 & 14 & 3 & 3 & 4 & 6 & 2 \\ class3 & 15 & 7 & 4 & 2 & 4 & 4 \\ class4 & 21 & 5 & 3 & 4 & 7 & 3 \end{bmatrix},$$

$$N^{t9}=\begin{bmatrix} & listen & write & talk & distraction & phone & sleep \\ class1 & 13 & 3 & 7 & 2 & 8 & 2 \\ class2 & 10 & 5 & 5 & 36 & 9 & 2 \\ class3 & 8 & 5 & 5 & 5 & 7 & 3 \\ class4 & 17 & 8 & 2 & 2 & 2 & 2 \end{bmatrix}.$$

Step 2. Calculate combination weights based on multi-class learning behavior matrices.

Step 1'. Based on the Eqs. (3) and (4), six learning behaviors entropy vectors of 9 time-points are obtained as follows

$$e_{t1}=\left[0.994,0.941,0.983,0.980,0.864,0.961\right],\ e_{t2}=\left[0.998,0.979,0.993,0.966,0.928,0.957\right],$$
$$e_{t3}=\left[0.999,0.986,0.953,0.918,0.933,0.913\right],\ e_{t4}=\left[0.994,0.960,0.985,0.987,0.977,0.856\right],$$
$$e_{t5}=\left[0.957,0.879,0.962,0.995,0.936,0.975\right],\ e_{t6}=\left[0.978,0.945,0.853,0.932,0.960,0.959\right],$$
$$e_{t7}=\left[0.985,0.926,0.963,0.968,0.993,0.843\right],\ e_{t8}=\left[0.990,0.966,0.968,0.975,0.986,0.968\right],$$
$$e_{t9}=\left[0.972,0.959,0.943,0.916,0.924,0.987\right].$$

Step 2'. Based on Eq. (5), six learning behaviors entropy weight vectors of 9 time-points are obtained as follows.

$$w_{t1}=\left[w_1,w_2,w_3,w_4,w_5,w_6\right] \quad w_{t2}=\left[w_1,w_2,w_3,w_4,w_5,w_6\right]$$
$$=\left[0.020,0.221,0.062,0.074,0.492,0.141\right],\ =\left[0.071,0.120,0.043,0.197,0.424,0.146\right],$$
$$w_{t3}=\left[w_1,w_2,w_3,w_4,w_5,w_6\right] \quad w_{t4}=\left[w_1,w_2,w_3,w_4,w_5,w_6\right]$$
$$=\left[0.004,0.046,0.158,0.275,0.225,0.292\right],\ =\left[0.025,0.174,0.063,0.054,0.099,0.585\right],$$
$$w_{t5}=\left[w_1,w_2,w_3,w_4,w_5,w_6\right] \quad w_{t6}=\left[w_1,w_2,w_3,w_4,w_5,w_6\right]$$
$$=\left[0.144,0.409,0.129,0.017,0.218,0.084\right],\ =\left[0.057,0.145,0.385,0.201,0.105,0.107\right],$$
$$w_{t7}=\left[w_1,w_2,w_3,w_4,w_5,w_6\right] \quad w_{t8}=\left[w_1,w_2,w_3,w_4,w_5,w_6\right]$$
$$=\left[0.045,0.231,0.115,0.099,0.023,0.499\right],\ =\left[0.068,0.234,0.217,0.170,0.093,0.217\right],$$

$$w_{t9} = \left[w_1, w_2, w_3, w_4, w_5, w_6\right] = \left[0.095, 0.138, 0.190, 0.280, 0.255, 0.042\right].$$

Therefore, based on entropy weight vectors of 9 time-points, each class comprehensive score vector of 9 time-points is obtained.

Step 3'. Based on the Eq.(6), calculate the comprehensive score of each class. Then, it gets

$$S_{t1} = \left[S_{11}, S_{12}, S_{13}, S_{14}\right]^{>} = \left[2.57, 4.56, 3.86, 3.30\right]^{>}, \quad S_{t2} = \left[S_{11}, S_{12}, S_{13}, S_{14}\right]^{>} = \left[4.79, 3.50, 4.69, 5.40\right]^{>}, \quad S_{t3} = \left[S_{11}, S_{12}, S_{13}, S_{14}\right]^{>} = \left[4.28, 4.47, 3.39, 1.69\right]^{>},$$

$$S_{t4} = \left[S_{11}, S_{12}, S_{13}, S_{14}\right]^{>} = \left[3.33, 3.98, 5.29, 3.22\right]^{>}, \quad S_{t5} = \left[S_{11}, S_{12}, S_{13}, S_{14}\right]^{>} = \left[7.75, 4.68, 5.04, 6.65\right]^{>}, \quad S_{t6} = \left[S_{11}, S_{12}, S_{13}, S_{14}\right]^{>} = \left[4.61, 2.94, 5.32, 3.53\right]^{>},$$

$$S_{t7} = \left[S_{11}, S_{12}, S_{13}, S_{14}\right]^{>} = \left[3.33, 3.17, 5.23, 3.68\right]^{>}, \quad S_{t8} = \left[S_{11}, S_{12}, S_{13}, S_{14}\right]^{>} = \left[4.76, 3.98, 5.11, 5.23\right]^{>}, \quad S_{t9} = \left[S_{11}, S_{12}, S_{13}, S_{14}\right]^{>} = \left[5.66, 6.65, 5.71, 4.25\right]^{>}.$$

Thus, the weight vector of each class of 9 time-points obtained by the entropy weight method is obtained as follows.

$$\omega_e^{t1} = \left[\omega_{e1}, \omega_{e2}, \omega_{e3}, \omega_{e4}\right]^{>} = \left[0.18, 0.32, 0.27, 0.23\right]^{>}, \quad \omega_e^{t2} = \left[\omega_{e1}, \omega_{e2}, \omega_{e3}, \omega_{e4}\right]^{>} = \left[0.26, 0.19, 0.25, 0.29\right]^{>}, \quad \omega_e^{t3} = \left[\omega_{e1}, \omega_{e2}, \omega_{e3}, \omega_{e4}\right]^{>} = \left[0.31, 0.32, 0.25, 0.12\right]^{>},$$

$$\omega_e^{t4} = \left[\omega_{e1}, \omega_{e2}, \omega_{e3}, \omega_{e4}\right]^{>} = \left[0.21, 0.25, 0.33, 0.20\right]^{>}, \quad \omega_e^{t5} = \left[\omega_{e1}, \omega_{e2}, \omega_{e3}, \omega_{e4}\right]^{>} = \left[0.32, 0.19, 0.21, 0.28\right]^{>}, \quad \omega_e^{t6} = \left[\omega_{e1}, \omega_{e2}, \omega_{e3}, \omega_{e4}\right]^{>} = \left[0.28, 0.18, 0.32, 0.22\right]^{>},$$

$$\omega_e^{t7} = \left[\omega_{e1}, \omega_{e2}, \omega_{e3}, \omega_{e4}\right]^{>} = \left[0.22, 0.21, 0.34, 0.24\right]^{>}, \quad \omega_e^{t8} = \left[\omega_{e1}, \omega_{e2}, \omega_{e3}, \omega_{e4}\right]^{>} = \left[0.25, 0.21, 0.27, 0.27\right]^{>}, \quad \omega_e^{t9} = \left[\omega_{e1}, \omega_{e2}, \omega_{e3}, \omega_{e4}\right]^{>} = \left[0.25, 0.30, 0.26, 0.19\right]^{>}.$$

Step 4'. Calculate the Pearson correlation coefficients of each learning behavior based on the learning behavior matrix *N*. Then, the Pearson correlation coefficient for each learned behavior is then obtained. For example, the Pearson correlation coefficient matric r^{t1} at time-point *t*1 is as follows.

$$r^{t1} = \begin{bmatrix} 1 & 0.97 & -0.99 & 0.15 & -0.74 & 0.38 \\ 0.97 & 1 & -0.95 & 0.22 & -0.84 & 0.37 \\ -0.99 & -0.95 & 1 & 0 & 0.80 & -0.52 \\ 0.15 & 0.22 & 0 & 1 & 0.17 & -0.82 \\ -0.74 & -0.84 & 0.80 & 0.17 & 1 & -0.70 \\ 0.38 & 0.37 & -0.52 & -0.82 & -0.70 & 1 \end{bmatrix}.$$

For ease of understanding, the Pearson correlation coefficients of the four classes at time point t1 are shown in Figure 5.

Thus, learning behavior indicator conflicts are obtained based on the Pearson correlation coefficient matric r^{t1}. For example, the learning behavior indicator conflicts R^{t1} at time-point *t*1 is obtained as follows.

$$R^{t1} = \begin{bmatrix} 0 & 0.03 & 1.99 & 0.85 & 1.74 & 0.62 \\ 0.03 & 0 & 1.95 & 0.78 & 1.84 & 0.63 \\ 1.99 & 1.95 & 0 & 1 & 0.20 & 1.52 \\ 0.85 & 0.78 & 1 & 0 & 0.83 & 1.82 \\ 1.74 & 1.84 & 0.20 & 0.83 & 0 & 1.70 \\ 0.62 & 0.63 & 1.52 & 1.82 & 1.70 & 0 \end{bmatrix}.$$

Then, the amount of information about learning behavior vectors at 9 time-points $\boldsymbol{C_t}(\boldsymbol{t} = \boldsymbol{t1}, \boldsymbol{t2}, \cdots, \boldsymbol{t9})$ are obtained as follows.

$$C_{t1} = \left[C_1, C_2, C_3, C_4, C_5, C_6\right] = \left[13.84, 9.57, 6.37, 4.30, 15.02, 3.15\right], \quad C_{t2} = \left[C_1, C_2, C_3, C_4, C_5, C_6\right] = \left[18.24, 6.64, 4.04, 9.76, 5.62, 1.88\right],$$

$$C_{t3}=\left[C_1,C_2,C_3,C_4,C_5,C_6\right] =\left[9.04,6.99,5.30,6.66,8.08,7.42\right], \quad C_{t4}=\left[C_1,C_2,C_3,C_4,C_5,C_6\right] =\left[19.01,12.52,3.63,2.82,6.60,12.50\right],$$

$$C_{t5}=\left[C_1,C_2,C_3,C_4,C_5,C_6\right] =\left[39.66,15.73,7.07,2.50,13.39,6.24\right], \quad C_{t6}=\left[C_1,C_2,C_3,C_4,C_5,C_6\right] =\left[28.02,7.39,13.93,4.20,11.51,1.98\right],$$

$$C_{t7}=\left[C_1,C_2,C_3,C_4,C_5,C_6\right] =\left[18.01,13.09,7.51,4.02,6.48,11.88\right], \quad C_{t8}=\left[C_1,C_2,C_3,C_4,C_5,C_6\right] =\left[12.54,8.98,8.90,5.35,6.25,5.07\right],$$

$$C_{t9}=\left[C_1,C_2,C_3,C_4,C_5,C_6\right] =\left[28.48,13.48,11.26,9.94,15.74,2.58\right].$$

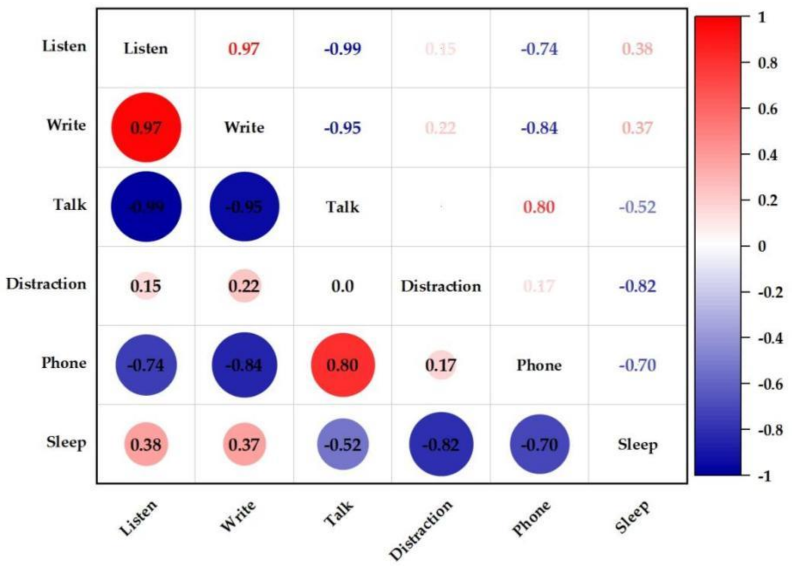

Figure 5. Pearson correlation coefficients of the four classes at time point $t1$.

Step 5'. The CRITIC weight of each behavior $w_{2j},(j=1,2,\cdots,6)$ is obtained based on Eq. (10). Then, the weight vectors by the CRITIC weight method is obtained as follows.

$$w_{t1}=\left[w_{21},w_{22},w_{23},w_{24},w_{25},w_{26}\right] =\left[0.100,0.100,0.127,0.101,0.121,0.120\right], \quad w_{t2}=\left[w_{21},w_{22},w_{23},w_{24},w_{25},w_{26}\right] =\left[0.395,0.144,0.088,0.211,0.122,0.041\right],$$

$$w_{t3}=\left[w_{21},w_{22},w_{23},w_{24},w_{25},w_{26}\right] =\left[0.208,0.161,0.122,0.153,0.186,0.171\right], \quad w_{t4}=\left[w_{21},w_{22},w_{23},w_{24},w_{25},w_{26}\right] =\left[0.333,0.219,0.064,0.049,0.116,0.219\right],$$

$$w_{t5}=\left[w_{21},w_{22},w_{23},w_{24},w_{25},w_{26}\right] =\left[0.496,0.186,0.084,0.030,0.158,0.074\right], \quad w_{t6}=\left[w_{21},w_{22},w_{23},w_{24},w_{25},w_{26}\right] =\left[0.418,0.110,0.208,0.063,0.172,0.030\right],$$

$$w_{t7}=\left[w_{21},w_{22},w_{23},w_{24},w_{25},w_{26}\right] =\left[0.295,0.215,0.123,0.066,0.106,0.195\right], \quad w_{t8}=\left[w_{21},w_{22},w_{23},w_{24},w_{25},w_{26}\right] =\left[0.266,0.191,0.189,0.114,0.133,0.108\right],$$

$$w_{t9}=\left[w_{21},w_{22},w_{23},w_{24},w_{25},w_{26}\right] =\left[0.350,0.165,0.138,0.122,0.193,0.032\right].$$

Step 6'. Based on the Eq.(11), calculate the comprehensive score of each class. It gets

$$S_{t1}=\left[S_{21},S_{22},S_{23},S_{24}\right]^{>} =\left[3.45,3.76,3.37,3.85\right]^{>}, \quad S_{t2}=\left[S_{21},S_{22},S_{23},S_{24}\right]^{>} =\left[10.82,8.69,9.53,12.59\right]^{>}, \quad S_{t3}=\left[S_{21},S_{22},S_{23},S_{24}\right]^{>} =\left[8.38,7.98,7.26,6.68\right]^{>},$$

$$S_{t4}=\left[S_{21},S_{22},S_{23},S_{24}\right]^{>} =\left[9.39,10.88,9.15,11.27\right]^{>}, \quad S_{t5}=\left[S_{21},S_{22},S_{23},S_{24}\right]^{>} =\left[11.71,6.89,8.25,13.47\right]^{>}, \quad S_{t6}=\left[S_{21},S_{22},S_{23},S_{24}\right]^{>} =\left[9.59,7.72,7.55,9.99\right]^{>},$$

$$S_{t7}=\left[S_{21},S_{22},S_{23},S_{24}\right]^{>} \quad S_{t8}=\left[S_{21},S_{22},S_{23},S_{24}\right]^{>} \quad S_{t9}=\left[S_{21},S_{22},S_{23},S_{24}\right]^{>}$$
$$=\left[7.92,5.80,7.06,8.17\right]^{>},=\left[7.24,6.33,7.27,8.82\right]^{>},=\left[7.86,7.55,6.37,8.24\right]^{>},$$

Thus, the weight vector of each class of 9 time-points by the CRITIC weight method is obtained as follows.

$$\omega_c^{t1}=\left[\omega_{c1}^{t1},\omega_{c2}^{t1},\omega_{c3}^{t1},\omega_{c4}^{t1}\right]^{>} \quad \omega_c^{t2}=\left[\omega_{c1}^{t2},\omega_{c2}^{t2},\omega_{c3}^{t2},\omega_{c4}^{t2}\right]^{>} \quad \omega_c^{t3}=\left[\omega_{c1}^{t3},\omega_{c2}^{t3},\omega_{c3}^{t3},\omega_{c4}^{t3}\right]^{>}$$
$$=\left[0.24,0.26,0.23,0.27\right]^{>},=\left[0.26,0.21,0.23,0.30\right]^{>},=\left[0.28,0.26,0.24,0.22\right]^{>},$$
$$\omega_c^{t4}=\left[\omega_{c1}^{t4},\omega_{c2}^{t4},\omega_{c3}^{t4},\omega_{c4}^{t4}\right]^{>} \quad \omega_c^{t5}=\left[\omega_{c1}^{t5},\omega_{c2}^{t5},\omega_{c3}^{t5},\omega_{c4}^{t5}\right]^{>} \quad \omega_c^{t6}=\left[\omega_{c1}^{t6},\omega_{c2}^{t6},\omega_{c3}^{t6},\omega_{c4}^{t6}\right]^{>}$$
$$=\left[0.23,0.27,0.22,0.28\right]^{>},=\left[0.29,0.17,0.20,0.33\right]^{>},=\left[0.28,0.22,0.22,0.29\right]^{>},$$
$$\omega_c^{t7}=\left[\omega_{c1}^{t7},\omega_{c2}^{t7},\omega_{c3}^{t7},\omega_{c4}^{t7}\right]^{>} \quad \omega_c^{t8}=\left[\omega_{c1}^{t8},\omega_{c2}^{t8},\omega_{c3}^{t8},\omega_{c4}^{t8}\right]^{>} \quad \omega_c^{t9}=\left[\omega_{c1}^{t9},\omega_{c2}^{t9},\omega_{c3}^{t9},\omega_{c4}^{t9}\right]^{>}$$
$$=\left[0.27,0.20,0.24,0.28\right]^{>},=\left[0.24,0.21,0.25,0.30\right]^{>},=\left[0.26,0.25,0.21,0.27\right]^{>}.$$

Step 7'. Based on Eq. (13), the weight vectors of four classes of 9 time-points by the combined weighting method are obtained as follows.

$$W^{t1}=\left[0.21,0.29,0.25,0.25\right]^{>},\ W^{t2}=\left[0.26,0.20,0.24,0.30\right]^{>},\ W^{t3}=\left[0.29,0.29,0.24,0.17\right]^{>},$$
$$W^{t4}=\left[0.22,0.26,0.28,0.24\right]^{>},\ W^{t5}=\left[0.31,0.18,0.21,0.30\right]^{>},\ W^{t6}=\left[0.28,0.20,0.27,0.25\right]^{>},$$
$$W^{t7}=\left[0.24,0.20,0.29,0.26\right]^{>},\ W^{t8}=\left[0.25,0.21,0.26,0.29\right]^{>},\ W^{t9}=\left[0.26,0.27,0.23,0.23\right]^{>},$$

Step 3. Construct SVNHFSs based on the Eqs. (14-16). Thus, the truth-membership hesitant degree is $\tilde{t}_q\ (q=1,2)$, the indeterminacy-membership hesitant degree is $\tilde{i}_q\ (q=1,2)$, and the falsity-membership is $\tilde{f}_q\ (q=1,2)$. Then, the SVNHFS $U_i^1\ (i=1,2,3,4)$ for four classes at time point $t1$ are as follows.

$$U_1^1=\left\langle \tilde{T}_1,\tilde{I}_1,\tilde{F}_1\right\rangle \quad U_2^1=\left\langle \tilde{T}_2,\tilde{I}_2,\tilde{F}_2\right\rangle$$
$$=\left\langle \{0.758\},\{0.091,.0.061\},\{0.030,0.061\}\right\rangle,=\left\langle \{0.600\},\{0.114,.0.086\},\{0.171,0.029\}\right\rangle,$$

$$U_3^1=\left\langle \tilde{T}_3,\tilde{I}_3,\tilde{F}_3\right\rangle \quad U_4^1=\left\langle \tilde{T}_4,\tilde{I}_4,\tilde{F}_4\right\rangle$$
$$=\left\langle \{0.548\},\{0.161,0.097\},\{0.161,0.032\}\right\rangle,=\left\langle \{0.730\},\{0.081,0.108\},\{0.054,0.027\}\right\rangle.$$

Specifically, SVNHZ classroom learning behaviors decision matrix values for four classes are shown in Table 1(a) and (b).

Table 1(a). SVNHZ time-based classroom learning behaviors decision matrix.

T \ Class	Class One	Class Two
t_1	<{0.758},{0.091,0.061},{0.030,0.061}>	<{0.600},{0.114,0.086},{0.171,0.029}>
t_2	<{0.667},{0.103,0.077},{0.103,0.051}>	<{0.636},{0.152,0.152},{0.030,0.030}>
t_3	<{0.644},{0.044,0.111},{0.133,0.067}>	<{0.628},{0.023,0.093},{0.140,0.116}>
t_4	<{0.730},{0.081,0.054},{0.081,0.054}>	<{0.714},{0.048,0.048},{0.119,0.071}>
t_5	<{0.643},{0.119,0.095},{0.095,0.048}>	<{0.400},{0.133,0.100},{0.233,0.133}>
t_6	<{0.576},{0.182,0.061},{0.152,0.030}>	<{0.630},{0.074,0.037},{0.222,0.037}>
t_7	<{0.538},{0.179,0.103},{0.154,0.026}>	<{0.483},{0.103,0.069},{0.241,0.103}>
t_8	<{0.528},{0.167,0.083},{0.167,0.056}>	<{0.531},{0.094,0.125},{0.188,0.063}>
t_9	<{0.457},{0.200,0.057},{0.229, 0.057}>	<{0.405},{0.135,0.162},{0.243, 0.054}>

Table 1(b). SVNHZ time-based classroom learning behaviors decision matrix.

T \ Class	Class Three	Class Four
t_1	<{0.548},{0.161,0.097},{0.161,0.032}>	<{0.730},{0.081,0.108},{0.054,0.027}>
t_2	<{0.538},{0.158,0.158},{0.079,0.053}>	<{0.696},{0.109,0.065},{0.087,0.043}>
t_3	<{0.667},{0.077,0.103},{0.077,0.077}>	<{0.829},{0.057,0.029},{0.057,0.029}>
t_4	<{0.579},{0.053,0.079},{0.132,0.158}>	<{0.791},{0.070,0.047},{0.070,0.023}>
t_5	<{0.441},{0.147,0.118},{0.176,0.118}>	<{0.732},{0.049,0.098},{0.049,0.073}>
t_6	<{0.412},{0.176,0.118},{0.235,0.059}>	<{0.743},{0.029,0.086},{0.086,0.057}>
t_7	<{0.472},{0.167,0.083},{0.139,0.139}>	<{0.676},{0.108,0.054},{0.135,0.027}>
t_8	<{0.611},{0.111,0.056},{0.111,0.111}>	<{0.605},{0.070,0.093},{0.163,0.070}>
t_9	<{0.394},{0.152,0.152},{0.212, 0.091}>	<{0.758},{0.061,0.061},{0.061, 0.061}>

Therefore, the SVNHZ time-based classroom learning behaviors decision matrix $\boldsymbol{U}$ is obtained. For example, the SVNHZ time-based classroom learning behaviors decision matrix $\boldsymbol{U^{t1}}$ at time-point $\boldsymbol{t1}$ is as follows.

$$
\begin{aligned}
U^1 &= \left[\left\langle \tilde{T}_1^1, \tilde{I}_1^1, \tilde{F}_1^1 \right\rangle, \left\langle \tilde{T}_2^1, \tilde{I}_2^1, \tilde{F}_2^1 \right\rangle, \left\langle \tilde{T}_3^1, \tilde{I}_3^1, \tilde{F}_3^1 \right\rangle, \left\langle \tilde{T}_4^1, \tilde{I}_4^1, \tilde{F}_4^1 \right\rangle\right] \\
&= \begin{bmatrix} \left\langle \{0.758\},\{0.091,0.061\},\{0.030,0.061\} \right\rangle, \left\langle \{0.600\},\{0.113,0.086\},\{0.171,0.029\} \right\rangle, \\ \left\langle \{0.548\},\{0.161,0.097\},\{0.161,0.032\} \right\rangle, \left\langle \{0.730\},\{0.081,0.108\},\{0.054,0.027\} \right\rangle. \end{bmatrix}.
\end{aligned}
$$

Step 4. Based on the combined time weights, the SVNHFWA operator is employed. Specifically, this study adopts the SVNHFWA operator to calculate the integrated value for each time point. Take the time point *t*1, for example, the collective SVNHFE $\boldsymbol{\phi_1}$ is obtained as follows.

$$
\begin{aligned}
\phi_1 &= SVNHFWA\left(U_1^1, U_2^1, U_3^1, U_4^1\right) = \sum_{n=1}^{4} W^{t1} \cdot U_n^1 \\
&= \bigcup_{\substack{\tilde{t}_1^1 \in \tilde{T}_1^1, \tilde{t}_2^1 \in \tilde{T}_2^1, \tilde{t}_3^1 \in \tilde{T}_3^1, \tilde{t}_4^1 \in \tilde{T}_4^1, \tilde{i}_{11}^1 \in \tilde{I}_1^1, \tilde{i}_{12}^1 \in \tilde{I}_1^1, \tilde{i}_{21}^1 \in \tilde{I}_2^1, \tilde{i}_{22}^1 \in \tilde{I}_2^1, \tilde{i}_{31}^1 \in \tilde{I}_3^1, \tilde{i}_{32}^1 \in \tilde{I}_3^1, \tilde{i}_{41}^1 \in \tilde{I}_4^1, \tilde{i}_{42}^1 \in \tilde{I}_4^1, \\ \tilde{f}_{11}^1 \in \tilde{F}_1^1, \tilde{f}_{12}^1 \in \tilde{F}_1^1, \tilde{f}_{21}^1 \in \tilde{F}_2^1, \tilde{f}_{22}^1 \in \tilde{F}_2^1, \tilde{f}_{31}^1 \in \tilde{F}_3^1, \tilde{f}_{32}^1 \in \tilde{F}_3^1, \tilde{f}_{41}^1 \in \tilde{F}_4^1, \tilde{f}_{42}^1 \in \tilde{F}_4^1.}} \left\{ \left\{ 1 - \prod_{q=1}^{4} \left(1 - \tilde{t}_q^1\right)^{W^{t1}} \right\}, \left\{ \prod_{q=1}^{4} \left(1 - \tilde{i}_q^1\right)^{W^{t1}} \right\}, \left\{ \prod_{q=1}^{4} \left(1 - \tilde{f}_q^1\right)^{W^{t1}} \right\} \right\} \\
&= \left\{ \begin{array}{l}
\left\{ 1 - (1-0.758)^{0.21} (1-0.600)^{0.29} (1-0.548)^{0.25} (1-0.730)^{0.25} \right\}, \\
\left\{ \begin{array}{l}
0.091^{0.21} 0.114^{0.29} 0.161^{0.25} 0.081^{0.25}, 0.091^{0.21} 0.114^{0.29} 0.161^{0.25} 0.108^{0.25}, \\
0.091^{0.21} 0.114^{0.29} 0.097^{0.25} 0.081^{0.25}, 0.091^{0.21} 0.114^{0.29} 0.097^{0.25} 0.108^{0.25}, \\
0.091^{0.21} 0.086^{0.29} 0.161^{0.25} 0.081^{0.25}, 0.091^{0.21} 0.086^{0.29} 0.161^{0.25} 0.108^{0.25}, \\
0.091^{0.21} 0.086^{0.29} 0.097^{0.25} 0.081^{0.25}, 0.091^{0.21} 0.086^{0.29} 0.097^{0.25} 0.108^{0.25}, \\
0.061^{0.21} 0.114^{0.29} 0.161^{0.25} 0.081^{0.25}, 0.061^{0.21} 0.114^{0.29} 0.161^{0.25} 0.108^{0.25}, \\
0.061^{0.21} 0.114^{0.29} 0.097^{0.25} 0.081^{0.25}, 0.061^{0.21} 0.114^{0.29} 0.097^{0.25} 0.108^{0.25}, \\
0.061^{0.21} 0.086^{0.29} 0.161^{0.25} 0.081^{0.25}, 0.061^{0.21} 0.086^{0.29} 0.161^{0.25} 0.081^{0.25}, \\
0.061^{0.21} 0.114^{0.29} 0.097^{0.25} 0.081^{0.25}, 0.061^{0.21} 0.114^{0.29} 0.097^{0.25} 0.108^{0.25}.
\end{array} \right\}, \\
\left\{ \begin{array}{l}
0.030^{0.21} 0.171^{0.29} 0.161^{0.25} 0.054^{0.25}, 0.030^{0.21} 0.171^{0.29} 0.161^{0.25} 0.027^{0.25}, \\
0.030^{0.21} 0.171^{0.29} 0.032^{0.25} 0.054^{0.25}, 0.030^{0.21} 0.171^{0.29} 0.032^{0.25} 0.027^{0.25}, \\
0.030^{0.21} 0.029^{0.29} 0.161^{0.25} 0.054^{0.25}, 0.030^{0.21} 0.029^{0.29} 0.161^{0.25} 0.027^{0.25}, \\
0.030^{0.21} 0.029^{0.29} 0.032^{0.25} 0.054^{0.25}, 0.030^{0.21} 0.029^{0.29} 0.032^{0.25} 0.027^{0.25}, \\
0.061^{0.21} 0.171^{0.29} 0.161^{0.25} 0.054^{0.25}, 0.061^{0.21} 0.171^{0.29} 0.161^{0.25} 0.027^{0.25}, \\
0.061^{0.21} 0.171^{0.29} 0.032^{0.25} 0.054^{0.25}, 0.061^{0.21} 0.171^{0.29} 0.032^{0.25} 0.027^{0.25}, \\
0.061^{0.21} 0.029^{0.29} 0.161^{0.25} 0.054^{0.25}, 0.061^{0.21} 0.029^{0.29} 0.161^{0.25} 0.027^{0.25}, \\
0.061^{0.21} 0.029^{0.29} 0.032^{0.25} 0.054^{0.25}, 0.061^{0.21} 0.029^{0.29} 0.032^{0.25} 0.027^{0.25}.
\end{array} \right\}
\end{array} \right\}.
\end{aligned}
$$

The time point $\boldsymbol{t_1}$ collective SVNHFE $\boldsymbol{U_1}$ is calculated as

$$U_1 = \left\{ \begin{array}{l} \{0.664\}, \\ \left\{ \begin{array}{l} 0.109, 0.117, 0.096, 0.103, \\ 0.100, 0.108, 0.088, 0.095, \\ 0.100, 0.107, 0.088, 0.095, \\ 0.092, 0.099, 0.081, 0.087. \end{array} \right\}, \left\{ \begin{array}{l} 0.088, 0.074, 0.059, 0.049, \\ 0.052, 0.044, 0.035, 0.029, \\ 0.102, 0.085, 0.068, 0.057, \\ 0.061, 0.051, 0.041, 0.034. \end{array} \right\} \end{array} \right\}.$$

Analogously, based on the aforementioned calculation steps, the other collective SVNHFE $\boldsymbol{U_i}\ (\boldsymbol{i = t_2, t_3, t_4, t_5, t_6})$ are derived as follows.

$$U_2 = \left\{ \begin{array}{l} \{0.646\}, \\ \left\{ \begin{array}{l} 0.126, 0.108, 0.126, 0, 108, \\ 0.126, 0.108, 0.126, 0.108, \\ 0.116, 0.100, 0.116, 0.100, \\ 0.116, 0.100, 0.116, 0.100, \end{array} \right\}, \left\{ \begin{array}{l} 0.072, 0.058, 0.065, 0.053, \\ 0.072, 0.058, 0.065, 0.053, \\ 0.060, 0.048, 0.054, 0.044, \\ 0.060, 0.048, 0.054, 0.044, \end{array} \right\} \end{array} \right\} U_3 = \left\{ \begin{array}{l} \{0.687\}, \\ \left\{ \begin{array}{l} 0.044, 0.039, 0, 047, 0.042, \\ 0.066, 0.058, 0.070, 0.063, \\ 0.057, 0.051, 0.061, 0.055, \\ 0.086, 0.077, 0.092, 0.082. \end{array} \right\}, \left\{ \begin{array}{l} 0.102, 0.091, 0.102, 0.091, \\ 0.097, 0.086, 0.097, 0.086, \\ 0.084, 0.075, 0.084, 0.075, \\ 0.079, 0.071, 0.079, 0.071. \end{array} \right\} \end{array} \right\}$$

$$U_4 = \left\{ \begin{array}{l} \{0.708\}, \\ \left\{ \begin{array}{l} 0.061, 0.055, 0.068, 0.062, \\ 0.061, 0.055, 0.068, 0.062, \\ 0.055, 0.050, 0.062, 0.056, \\ 0.055, 0.050, 0.062, 0.056. \end{array} \right\}, \left\{ \begin{array}{l} 0.099, 0.076, 0.104, 0.080, \\ 0.087, 0.066, 0.091, 0.070, \\ 0.091, 0.069, 0.095, 0.073, \\ 0.079, 0.061, 0.083, 0.064. \end{array} \right\} \end{array} \right\} U_5 = \left\{ \begin{array}{l} \{0.605\}, \\ \left\{ \begin{array}{l} 0.097, 0.120, 0.092, 0.114, \\ 0.092, 0.114, 0.088, 0.108, \\ 0.090, 0.112, 0.086, 0.107, \\ 0.086, 0.106, 0.082, 0.101. \end{array} \right\}, \left\{ \begin{array}{l} 0.104, 0.117, 0.096, 0.108, \\ 0.094, 0.106, 0.086, 0.097, \\ 0.084, 0.095, 0.078, 0.088, \\ 0.076, 0.086, 0.070, 0.079. \end{array} \right\} \end{array} \right\}$$

$$U_6 = \left\{ \begin{array}{l} \{0.602\}, \\ \left\{ \begin{array}{l} 0.095, 0.125, 0.085, 0.112, \\ 0.083, 0.109, 0.074, 0.097, \\ 0.070, 0.092, 0.063, 0.083, \\ 0.061, 0.080, 0.055, 0.072 \end{array} \right\}, \left\{ \begin{array}{l} 0.160, 0.144, 0.110, 0.099, \\ 0.112, 0.101, 0.077, 0.069, \\ 0.102, 0.092, 0.070, 0.063, \\ 0.071, 0.064, 0.049, 0.044. \end{array} \right\} \end{array} \right\} U_7 = \left\{ \begin{array}{l} \{0.552\}, \\ \left\{ \begin{array}{l} 0.137, 0.115, 0.112, 0.094, \\ 0.127, 0.106, 0.103, 0.086, \\ 0.120, 0.100, 0.098, 0.082, \\ 0.111, 0.092, 0.090, 0.075. \end{array} \right\}, \left\{ \begin{array}{l} 0.158, 0.104, 0.158, 0.104, \\ 0.133, 0.087, 0.133, 0.087, \\ 0.102, 0.067, 0.102, 0.067, \\ 0.086, 0.057, 0.086, 0.057. \end{array} \right\} \end{array} \right\}$$

$$U_8 = \left\{ \begin{array}{l} \{0.574\}, \\ \left\{ \begin{array}{l} 0.104, 0.113, 0.087, 0.095, \\ 0.110, 0.120, 0.093, 0.100, \\ 0.087, 0.095, 0.073, 0.080, \\ 0.093, 0.101, 0.078, 0.085. \end{array} \right\}, \left\{ \begin{array}{l} 0.153, 0.120, 0.153, 0.120, \\ 0.121, 0.095, 0.121, 0.095, \\ 0.117, 0.092, 0.117, 0.092, \\ 0.093, 0.073, 0.093, 0.073. \end{array} \right\} \end{array} \right\} U_9 = \left\{ \begin{array}{l} \{0.527\}, \\ \left\{ \begin{array}{l} 0.128, 0.128, 0.128, 0.128, \\ 0.134, 0.134, 0.134, 0.134, \\ 0.092, 0.092, 0.092, 0.092, \\ 0.097, 0.097, 0.097, 0.097. \end{array} \right\}, \left\{ \begin{array}{l} 0.168, 0.168, 0.138, 0.138, \\ 0.111, 0.111, 0.091, 0.091, \\ 0.117, 0.117, 0.096, 0.096, \\ 0.078, 0.078, 0.064, 0.064. \end{array} \right\} \end{array} \right\}$$

Step 5. The cosine measure values for time-based classes SVNHFE are calculated concerning the ideal element $\boldsymbol{U^* =< 1, 0, 0 >}$ by Eq. (2) and the non-ideal element $\boldsymbol{U^- =< 0, 0, 1 >}$ by Eq. (16). Therefore, the cosine measure values between $\boldsymbol{U_i}\ (\boldsymbol{i = 1, 2, \cdots, 9})$ and $\boldsymbol{U^*}$ are obtained as follows.

$$\cos\left(U_1, U^*\right) = 0.986, \cos\left(U_2, U^*\right) = 0.982, \cos\left(U_3, U^*\right) = 0.988,$$
$$\cos\left(U_4, U^*\right) = 0.990, \cos\left(U_5, U^*\right) = 0.976, \cos\left(U_6, U^*\right) = 0.980,$$
$$\cos\left(U_7, U^*\right) = 0.968, \cos\left(U_8, U^*\right) = 0.970, \cos\left(U_9, U^*\right) = 0.959.$$

The cosine measure values between $\boldsymbol{U_i}\ (\boldsymbol{i = t_2, t_3, t_4, t_5, t_6})$ and $\boldsymbol{U^-}$ are obtained as follows.

$$\cos\left(U_1, U^-\right) = 0.086, \cos\left(U_2, U^-\right) = 0.086, \cos\left(U_3, U^-\right) = 0.123,$$
$$\cos\left(U_4, U^-\right) = 0.113, \cos\left(U_5, U^-\right) = 0.148, \cos\left(U_6, U^-\right) = 0.145,$$
$$\cos\left(U_7, U^-\right) = 0.174, \cos\left(U_8, U^-\right) = 0.183, \cos\left(U_9, U^-\right) = 0.196.$$

Step 6. Based on the cosine measure values, the optimal learning effects of the 9 time-points of the classes are ranked as $\boldsymbol{U_4 \succ U_3 \succ U_1 \succ U_2 \succ U_6 \succ U_5 \succ U_8 \succ U_7 \succ U_9}$**,** and the worst learning effects of the 9 time-points of the classes are ranked as $\boldsymbol{U_9 \succ U_8 \succ U_7 \succ U_5 \succ U_6 \succ U_3 \succ U_4 \succ U_1 \sim U_2}$**.**

4.3 Comprehensive Analysis and Discussion

To confirm the feasibility and utility of the proposed method in assessing the effectiveness of student learning, this study conducted a comparative analysis with the classical entropy weight method and the CRITIC method [38, 39]. The positive and negative cosine measurement value by the classical entropy weight method and the classical CRITIC weight method is shown in Table 2.

Table 2. The proposed weighting method ranking results.

Time-points	The classical entropy weight method		The classical CRITIC weight method	
	Positive cosine measurement value	Negative cosine measurement value	Positive cosine measurement value	Negative cosine measurement value
t1	0.985	0.090	0.987	0.082
t2	0.981	0.087	0.982	0.086
t3	0.987	0.131	0.990	0.115
t4	0.989	0.121	0.991	0.105
t5	0.975	0.151	0.977	0.144
t6	0.977	0.153	0.982	0.138
t7	0.966	0.182	0.970	0.167
t8	0.970	0.183	0.970	0.183
t9	0.953	0.209	0.964	0.185

For convenience, the radar map of positive and negative cosine measurement values of the three methods are shown in Figures 6 and 7.

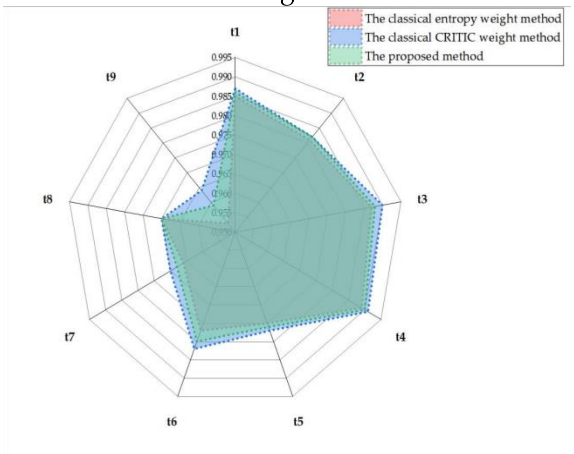

Figure 6. Radar map of the positive cosine measurement value.

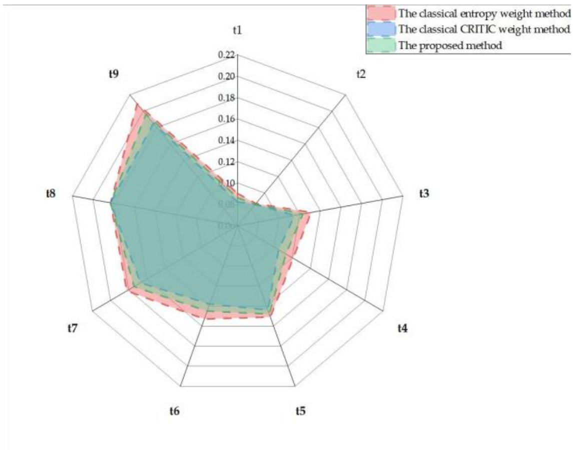

Figure 7. Radar map of the negative cosine measurement value.

Besides, the different weight method ranking results are shown in Table 3.

Table 3. Different weight method ranking results.

Method	Positive Sorting results	Negative Sorting results	Optimal time-point	Worst time-point
The proposed method	$U_4 \succ U_3 \succ U_1 \succ U_2 \succ U_6 \succ U_5 \succ U_8 \succ U_7 \succ U_9$	$U_9 \succ U_8 \succ U_7 \succ U_5 \succ U_6 \succ U_3 \succ U_4 \succ U_1 \sim U_2$.	U_4	U_9
The classical entropy weight method	$U_4 \succ U_3 \succ U_1 \succ U_2 \succ U_6 \succ U_5 \succ U_8 \succ U_7 \succ U_9$	$U_9 \succ U_8 \succ U_7 \succ U_6 \succ U_5 \succ U_1 \succ U_4 \succ U_3 \succ U_2$.	U_4	U_9
The classical CRITIC weight method	$U_4 \succ U_3 \succ U_1 \succ U_6 \succ U_2 \succ U_5 \succ U_8 \succ U_7 \succ U_9$	$U_9 \succ U_8 \succ U_7 \succ U_5 \succ U_6 \succ U_3 \succ U_4 \succ U_2 \succ U_1$.	U_4	U_9

The comparison reveals that the class learning effectiveness of 9 time-points order obtained by the proposed method aligns with the ranking results obtained from the classical methods. They all consider $\boldsymbol{U_4}$ as the ideal time-point and $\boldsymbol{U_9}$ as the non-ideal time-point.

Therefore, based on students' classroom behavior at different time-points under the sorting results, teachers dynamically adjust teaching strategies to enhance engagement and improve learning outcomes. By promptly addressing attention lapses or low participation, teachers can modify content, and methods, or introduce interactive activities to re-engage students. This adaptive approach ensures personalized pacing and difficulty adjustments, optimizing overall teaching effectiveness and fostering student development.

Then, to further establish the effectiveness and practicality of the proposed TQE method, this study engages in a comparative assessment against alternative methodologies, including the traditional cosine measurement method, as well as the SVNHF normalized Hamming distance, the SVNHF normalized Euclidean distance, and their corresponding similarity measures [40-42]. Specifically, the sorting results for the proposed method and other alternative methods are shown in Table 4. Among them, in Table 4, which are consistent with those of existing methods. They all agree that time-point $\boldsymbol{U_4}$ is the optimal scheme. Based on this consistency, the proposed method is effective and reliable.

Table 4. Different MADM method ranking results.

Method	**Positive Sorting results**	**Optimal time-point**	**Worst time-point**
The proposed method	$U_4 \succ U_3 \succ U_1 \succ U_2 \succ U_6 \succ U_5 \succ U_8 \succ U_7 \succ U_9$	U_4	U_9
The traditional cosine measurement method	$U_4 \succ U_3 \succ U_1 \succ U_2 \succ U_6 \succ U_5 \succ U_8 \succ U_7 \succ U_9$	U_4	U_9
The SVNHF normalized Hamming distance measurement method	$U_4 \succ U_3 \succ U_1 \succ U_2 \succ U_6 \succ U_5 \succ U_8 \succ U_7 \succ U_9$	U_4	U_9
The SVNHF normalized Euclidean Distance measurement method	$U_4 \succ U_3 \succ U_1 \succ U_2 \succ U_6 \succ U_5 \succ U_8 \succ U_7 \succ U_9$	U_4	U_9
The similarity measures based on SVNHF normalized Euclidean Distance	$U_4 \succ U_3 \succ U_1 \succ U_2 \succ U_6 \succ U_5 \succ U_8 \succ U_7 \succ U_9$	U_4	U_9
The similarity measures based on SVNHF normalized Euclidean Distance	$U_4 \succ U_3 \succ U_1 \succ U_2 \succ U_6 \succ U_5 \succ U_8 \succ U_7 \succ U_9$	U_4	U_9

Based on the aforementioned, the proposed TQE method for higher education effectively integrates machine vision technology with SVNHFS, providing a novel framework for assessing educational quality. However, several limitations still exist, particularly regarding generalization and broader applicability. First, the proposed method is constrained by the precision of classroom cameras. The limited resolution and accuracy may lead to misidentifications during the recognition process, potentially affecting the overall reliability of the evaluation. Moreover, this reliance on specific camera setups may limit the method's generalization to other educational environments with different technological infrastructures or larger, more complex datasets, making it challenging to apply the approach universally. Second, the approach depends on predefined evaluation indicators, which may not fully capture the dynamic and diverse nature of classroom interactions. This limitation reduces its ability to adapt to varied classroom settings and teaching styles. Third, while SVNHFS offers flexibility in handling uncertain data, its complexity may impede real-time processing and large-scale implementation, particularly when applied to extensive datasets. This highlights the need for further refinement to enhance computational efficiency and scalability.

As the future direction, the research could explore the adaptation of this model to different set structures. For instance, the current approach could be extended to evaluate more dynamic and heterogeneous educational environments, such as online learning platforms or vocational training programs. Additionally, the incorporation of multi-dimensional data structures—such as temporal sequences or multi-class behavior matrices—may reveal further insights into student learning patterns. By broadening the future directions, the proposed framework could be applied to more complex or larger datasets, enhancing its generalizability and utility. Exploring these applications would emphasize the wider implications of this study and potentially lead to more robust, versatile educational evaluation tools.

5. Conclusions

To mitigate the subjectivity inherent in teaching quality assessments and to promote greater automation and intelligence in the evaluation process, this study proposes a method for assessing the quality of university classroom education within machine vision and SVNHF environments. The main conclusions of this study are as follows.

First, the YOLOv5 deep learning object detection algorithm is employed to identify student behaviors in the classroom, thereby constructing a classroom behavior matrix. This approach enhances the objectivity of behavior detection and provides a robust foundation for TQE in higher education.

Second, a weighting method combining the entropy weight method and the CRITIC method is introduced to calculate the weights at different time points. This method replaces the traditional subjective weighting process, and reduces the limitations of single-method weighting, thereby making the evaluation results more objective and effective.

Third, this study constructs a time-based SVNHF evaluation matrix, which is weighted using the SVNHFWA operator. Additionally, this study introduces the cosine measurement method to rank the optimal and worst learning effectiveness time points, respectively. Through this evaluation method, teachers dynamically adjust teaching strategies, and students adjust their learning state in time to improve efficiency.

Last, the effectiveness and feasibility of the proposed evaluation model are demonstrated through a case study. Additionally, comparisons with the classical entropy weight method and CRITIC weight method confirm the validity of the combined weighting approach introduced in this study. Moreover, consistent results are obtained when compared with various MADM methods, further validating the robustness of the proposed decision-making framework.

However, the proposed TQE method offers a novel framework for classroom evaluation, but limitations remain. Camera resolution and setup may impact reliability, and reliance on predefined indicators reduces adaptability. The complexity of SVNHFS also affects scalability. Future work could enhance generalizability by adapting the model to diverse environments, incorporating multi-dimensional data, and applying it to larger datasets for broader insights.

Funding: Fangwei Zhang's work is partially supported by the Special Key Project of the Planning of Shandong Science of Education on Innovation Literacy. (Titled: Research on the integration mechanism of innovation and entrepreneurship education and professional education in application-oriented universities under OBE mode, No. 2022CZD016)

Conflicts of Interest: The authors declare no conflict of interest.

Data and source code available statement: The data and the source code that support the findings of this study are available on request from the corresponding author Mingjie Li upon reasonable request.

References

1. Wang, S., Wang, F., Zhu, Z., Wang, J., Tran, T., Du, Z. Artificial intelligence in education: A systematic literature review. *Expert. Syst. Appl.*, **2024**, 252, 124167. DOI: 10.1016/j.eswa.2024.124167.
2. Fialho, I., Cid, M., Coppi, M. Grounding and improving assessment in higher education: a way of promoting quality education. *In Frontiers in Education*, **2023**, 8, 1143356. DOI: 10.3389/feduc.2023.1143356.
3. Dou, W. MADM framework based on the triangular Pythagorean fuzzy sets and applications to college public English teaching quality evaluation. *J. Intell. Fuzzy. Syst.*, **2023**, 45, 4395-4414.

4. Liu, C.F., Luo, Y.S. New aggregation operators of single-valued neutrosophic hesitant fuzzy set and their application in multi-attribute decision making. *Pattern. Anal. Appl.*, **2019**, 22, 417–427. DOI: 10.1007/s10044-017-0635-6.
5. Arasteh, H., MahmodiRad, M. Effective teaching: an approach based on evaluation of instruction by students. *Koomesh*, **2024**, 5(2), 1-8.
6. Roxå, T., Ahmad, A., Barrington, J., Van Maaren, J., Cassidy, R. Reconceptualizing student ratings of teaching to support quality discourse on student learning: a systems perspective. *High. Educ.*, **2021**, 1-21. DOI: 10.1007/s10734-020-00615-1.
7. Li, C. Simulation of University Teaching Achievement Evaluation Based on Deep Learning and Improved Vector Machine Algorithm. *Appl. Artif. Intell.*, **2023**, 37, 2195221. DOI: 10.1080/08839514.2023.2195221.
8. Li, D. An interactive teaching evaluation system for preschool education in universities based on machine learning algorithm. *Comput. Hum. Behav.*, **2024**, 157, 108211. DOI: 10.1016/j.chb.2024.108211.
9. Li, Y., Zhang H. Big data technology for teaching quality monitoring and improvement in higher education-joint K-means clustering algorithm and Apriori algorithm. *Systems and Soft Computing*, **2024**, 6, 200125. DOI: 10.1016/j.sasc.2024.200125.
10. Xia, F. Optimized multiple-attribute group decision-making through employing probabilistic hesitant fuzzy TODIM and EDAS technique and application to teaching quality evaluation of international Chinese course in higher vocational colleges. *Heliyon,* **2024**, 10, e25758. DOI: 10.1016/j.heliyon.2024.e25758.
11. Almufarreh A., Noaman K.M., Saeed M.N. Academic Teaching Quality Framework and Performance Evaluation Using Machine Learning. *Appl. Sci.,* **2023**, 13, 3121. DOI: 10.3390/app13053121.
12. Cui, Y. Optimizing decision trees for English Teaching Quality Evaluation (ETQE) using Artificial Bee Colony (ABC) optimization. *Heliyon,* **2023**, 9, e19274. DOI: 10.1016/j.heliyon.2023.e19274.
13. Li, F., Wang C. Artificial intelligence and edge computing for teaching quality evaluation based on 5G-enabled wireless communication technology. *J. Cloud. Comput*., **2023**, 12, 45. DOI: 10.1186/s13677-023-00418-6.
14. Zhao, Y., Li, W., Jiang, H., Siyiti, M., Zhao, M., You, S., Li, Y., Yan, P. Development of a blended teaching quality evaluation scale (BTQES) for undergraduate nursing based on the Context, Input, Process and Product (CIPP) evaluation model: A cross-sectional survey. *Nurse. Educ. Pract*., **2024**, 77, 103976. DOI: 10.1016/j.nepr.2024.103976.
15. Ren, P., Yang, L., Luo, F. Automatic scoring of student feedback for teaching evaluation based on aspect-level sentiment analysis. *Educ. Inf. Technol*., 2023, 28(1), 797-814.
16. Saha, A., Deli, I., and Broumi, S. Hesitant triangular neutrosophic numbers and their applications to MADM. *Neutrosophic Sets and Systems*, **2020**, 35, 269-298.
17. Biswas, P., Pramanik, S., Giri, B. C. TOPSIS method for multi-attribute group decision-making under single-valued neutrosophic environment. *Neural. Comput. Appl.*, **2016**, 27, 727-737.
18. Deli, I.; Şubaş, Y. A ranking method of single valued neutrosophic numbers and its applications to multi-attribute decision making problems. *International journal of machine learning and cybernetics,* **2017**, 8, 1309-1322.
19. Mohamed, M., Metwaly, A. A., Ibrahim, M., Smarandache, F., and Voskoglou, M. Partnership of Lean Six Sigma and Digital Twin under Type 2 Neutrosophic Mystery Toward Virtual Manufacturing Environment: Real Scenario Application. *Sustainable Machine Intelligence Journal,* **2024**, 8, 6-99.
20. Saqlain, M., Garg, H., Kumam, P., and Kumam, W. Uncertainty and decision-making with multi-polar interval-valued neutrosophic hypersoft set: A distance, similarity measure and machine learning approach. *Alex. Eng. J*., **2023**, 84, 323-332.
21. Smarandache, F. Foundation of the SuperHyperSoft Set and the Fuzzy Extension SuperHyperSoft Set: A New Vision. *Neutrosophic Systems with Applications*, **2023**, 11, 48-51.
22. Zhao, M. and Ye, J. MADM Technique Using Tangent Trigonometric SvNN Aggregation Operators for the Teaching Quality Assessment of Teachers. *Neutrosophic Sets and Systems,* **2023**, 50, 652-662.`
23. Ye, J. Multiple-attribute decision-making method under a single-valued neutrosophic hesitant fuzzy environment. *Int. J. Intell. Syst*., **2015**, 24, 23-36.
24. Saeed, M., Kareem, K., Razzaq, F., and Saqlain, M. Unveiling Efficiency: Investigating Distance Measures in Wastewater Treatment Using Interval-Valued Neutrosophic Fuzzy Soft Set. *Neutrosophic Systems with Applications*, **2024**, 15, 1-15.

25. El-Douh, A., Lu, S., Abdelhafeez, A., and Aziz, A. A Neutrosophic Multi-Criteria Model for Evaluating Sustainable Soil Enhancement Methods and their Cost Implications in Construction. *Sustainable Machine Intelligence Journal*, **2023**, 5, 1-1.
26. Zhong, Y. Evaluation and analysis of teaching quality of university teachers using machine learning algorithms. *J. Intell. Syst*., **2023**, 32, 20220204. DOI: 10.1515/jisys-2022-0204.
27. Tzampazaki, M., Zografos, C., Vrochidou, E., and Papakostas, G. A. Machine Vision—Moving from Industry 4.0 to Industry 5.0. *Appl. Sci.*, **2024**, 14(4), 1471. DOI: 10.3390/app14041471.
28. Manakitsa, N., Maraslidis, G. S., Moysis, L., and Fragulis, G. F. A review of machine learning and deep learning for object detection, semantic segmentation, and human action recognition in machine and robotic vision. *Technologies*, **2024**, 12(2), 15. DOI: 10.3390/technologies12020015.
29. Bai, T., Gao, J., Yang, J., and Yao, D. A study on railway surface defects detection based on machine vision. *Entropy*, **2021**, 23(11), 1437. DOI: 10.3390/e23111437.
30. Zhang, H., Wang, Z., Guo,Y., Ma, Y., Cao, W., Chen, D., Yang, S., and Gao, R. Weed Detection in Peanut Fields Based on Machine Vision. *Agriculture*, **2022**, 12, 1541. DOI: 10.3390/agriculture12101541.
31. Li, J., Zhang, F., Wang, R., Ni, H., Li, T. A comprehensive evaluation model for university classroom teaching quality based on machine vision and Fermatean fuzzy sets. *Soft. Comput.*, **2023**, 1-14.
32. Bai, G. Simulation of performance skills teaching system based on machine vision and sensor audio signal processing. *Measurement: Sensors*, **2024**, 33, 101224. DOI: 10.1016/j.measen.2024.101224.
33. Cheng, Y. Video-based student classroom classroom behavior state analysis. I*nternational Journal of Education and Humanities*, **2022**, 5(2), 229-233.
34. Goldberg, P.; Sümer, Ö.; Stürmer, K.; Wagner, W., Göllner, R., Gerjets, P., Trautwein, U. Attentive or not? Toward a machine learning approach to assessing students' visible engagement in classroom instruction. *Educ. Psychol. Rev*., **2021**, 33, 27-49.
35. Ye, J. Multi-criteria decision-making method using the correlation coefficient under single-valued neutrosophic environment. *Int. J. Gen. Syst*., **2013**, 42, 386-394.
36. Jose M. N., Valerio A. P. S., Miguel A. O., Antonella P. M. Compatibility and correlation of multi-attribute decision making: a case of industrial relocation. *Ann. Oper. Res*., **2023**, 326 831-852.
37. Yu, W.; Zhou, P.; Shu, L.; Wei, S.; Jiang, C.; Zheng, H. Research progress on the human behavior recognition based on machine learning methods. *Recent Patents on Mechanical Engineering,* **2023**, 16, 32-44.
38. Zhou, M., Liu, X. B., Chen, Y. W., Qian, X. F., Yang, J. B., and Wu, J. Assignment of attribute weights with belief distributions for MADM under uncertainties. *Knowl-Based. Syst*., **2020**, 189, 105110. DOI: 10.1016/j.knosys.2019.105110.
39. Sun, H., Wei, G. W., Chen, X. D., and Mo, Z. W. Extended EDAS method for multiple attribute decision making in mixture z-number environment based on CRITIC method. *J. Intell. Fuzzy. Syst.*, **2022**, 43(3), 2777-2788.
40. Riaz, M., Almalki, Y., Batool, S., and Tanveer, S. Topological structure of single-valued neutrosophic hesitant fuzzy sets and data analysis for uncertain supply chains. *Symmetry*, **2022**, 14(7), 1382. DOI: 10.3390/sym14071382.
41. Şahin, R. Neutrosophic QUALIFLEX based on neutrosophic hesitancy index for selecting a potential antivirus mask supplier over COVID-19 pandemic. *Soft*. *Comput*., **2022**, 26(19), 10019-10033.
42. Sahin, R.; Liu, P. E. I. D. E. Distance and Similarity Measures for Multiple Attribute Decision Making with Single-Valued Neutrosophic Hesitant Fuzzy Information. In New Trends in Neutrosophic Theory and Applications; Smarandache, F., Ed.; Pons Editions: Brussells, Belgium, 2016; pp. 35–54.

Received: July 26, 2024. Accepted: Oct 24, 2024